For reprint orders, please contact: reprints@futuremedicine.com

Nanomedicine



Optimizing enzyme-responsive polymersomes for protein-based therapies

Dorian Foster¹, Alaura Cakley¹ & Jessica Larsen*,1,2

¹Department of Chemical & Biomolecular Engineering, Center for Nanotherapeutic Strategies in the Central Nervous System, Clemson University, Clemson, SC 29631, USA

²Department of Bioengineering, Center for Nanotherapeutic Strategies in the Central Nervous System, Clemson University, Clemson, SC 29631, USA

*Author for correspondence: larsenj@clemson.edu

Aims: Stimuli-responsive polymersomes are promising tools for protein-based therapies, but require deeper understanding and optimization of their pathology-responsive behavior. Materials & methods: Hyaluronic acid (HA)-poly(b-lactic acid) (PLA) polymersomes self-assembled from block copolymers of varying molecular weights of HA were compared for their physical properties, degradation and intracellular behavior. Results: Major results showed increasing enzyme-responsivity associated with decreasing molecular weight. The major formulation differences were as follows: the HA(5 kDa)-PLA formulation exhibited the most pronounced release of encapsulated proteins, while the HA(7 kDa)-PLA formulation showed the most different release behavior from neutral. Conclusion: We have discovered design rules for HA-PLA polymersomes for protein delivery, with lower molecular weight leading to higher encapsulation efficiency, greater release and greater intracellular uptake.

First draft submitted: 16 October 2023; Accepted for publication: 20 November 2023; Published online: 25 January 2024

Keywords: biodegradable • drug delivery • hyaluronic acid • polymer science • polymersomes • protein therapy • stimuli-responsive release

Proteins are complex and diverse biomolecules that serve distinct and essential bodily functions [1]. Protein-based therapies have become widespread for disease management across many affected organs. Owing to their intricate structures, proteins can serve complex sets of functions that traditional small-molecule drugs cannot [1]. Protein-based therapies encompass simple protein supplementation or replacement as well as augmentation of existing biological pathways or interference with problematic molecules. These therapies often come at lower development costs as well as with lower risks of side effects than small-molecule drug combinations that would be required to accomplish comparable effects [1,2], leading to more rapid clinical translation and approval [3].

Although protein-based therapies show great promise for addressing the complicated mechanisms and manifestations of disease, protein delivery can be a major challenge. Traditional, patient-friendly drug administration routes are unviable for protein therapy. For example, proteins cannot be administered orally because they are easily digested in the gastrointestinal tract; bioavailability is also an issue for pulmonary or nasal administration, as some proteins are too large to traverse the necessary membranes [4]. Intravenous administration avoids these issues, but proteins are not always soluble or stable enough for direct administration [2]. Additionally, intravenous administration is systemic, distributing the protein to many tissues and organs through the entirety of the circulatory system. When a disease is localized to a specific organ system or tumor site, whole-body administration may have low efficacy. One method that addresses these challenges is to use targeted nanoparticles to enable the site-specific delivery of proteins or enzymes via intravenous injections [4].

Polymersomes (PSs) are one such nanoparticle carrier that have generated much interest as controlled drug-delivery systems; toward the goal of this paper, PSs have demonstrated the ability to encapsulate and protect biologics, including proteins and enzymes, for therapeutic delivery [5,6]. PSs are nano-sized vesicles that self-assemble in an aqueous solution from amphiphilic block copolymers permitting the weight fraction of the hydrophilic fraction (f) is between 25 and 40% [7]. Because of the bilayer structure, PSs can encapsulate hydrophilic and hydrophobic drugs.



Choice of polymers, polymer molecular weight (MW) and synthesis conditions can all influence PS properties such as size, morphology and surface charge, which can all impact loading capacity and cellular transport [7]. Additionally, the ease and versatility of chemical modification make PSs attractive for targeted drug delivery by introducing stimuli-responsive drug release. Stimuli-responsive drug-delivery systems release their payload only upon exposure to pathological conditions, the benefits of which are greater drug efficacy and reduction of off-target effects [8–11]. PSs are well suited for use as stimuli-responsive drug systems owing to the tunable nature of polymers, which can be modified to respond to specific stimuli. Enzymes are attractive chemical stimuli because dysregulation of specific enzyme levels has been associated with a variety of diseases [12]. Additionally, enzymes are known to catalyze certain chemical reactions and are often substrate-specific [13], making them suitable for controlled delivery that is reaction-based. In tandem with stimuli-responsive targeting, facile functionalization of the PS surface enables the attachment of targeting ligands associated with specific tumors, organs and lesions [14–18]. Here, we have leveraged these abilities of PSs to develop enzyme-responsive protein-based therapies.

We have developed a hyaluronidase (HYAL)-responsive PS-based system for localized protein delivery to diseased organs or cells. The HYAL family of enzymes is primarily responsible for the degradation of hyaluronic acid (HA). HYAL is naturally found in different forms throughout major organs and bodily fluids. Its pathological upregulation has been observed in various cancers [19–21], some lysosomal storage disorders [5,22] and broadly in conditions associated with inflammation [23] and injury [24]. Because of its widespread dysregulation associated with disease, HYAL is a useful target for designing an enzyme-responsive drug-delivery system with HYAL-triggered release. Several of the human isoforms of HYAL are most active under acidic conditions [23,25] so we sought to dually integrate pH-responsivity as a secondary release mechanism for our design to further enable HYAL activity. Some of the conditions associated with upregulated HYAL are also linked to acidic environments; for example, acidity is a defining aspect of the microenvironment of cancerous tumors [26–28] and also of lysosomes [29], the cellular organelles affected by lysosomal storage disorders (LSDs). Therefore pH responsivity makes this system dually responsive to specific disease pathologies. With these goals in mind, we selected HA and poly(b-lactic acid) (PLA) as promising polymer blocks for PSs with responsivity to HYAL as well as to pH, respectively [30].

In the HA–PLA block copolymer, HA serves as the hydrophilic block while PLA serves as the hydrophobic block. PLA has already received US FDA approval in various biomedical applications [31,32], while HA is a biopolymer that is made by the body [33–35], making the copolymer highly biocompatible. Structurally, HA–PLA is very similar to PEG–PLA, which has been a popular approach to PS drug-delivery systems due to the wide use of PEG to enhance circulation half-lives in other FDA-approved nanoparticle systems, like the COVID-19 vaccine [36]. Despite its successes, PEG is susceptible to increased clearance rates and immune response with repeated exposure in the body due to antibody development [31,32]. HA may be able to overcome these challenges while simultaneously serving as a responsive component of the system. As a copolymer, HA–PLA has been previously reported to self-assemble as PSs by our group and others [22,37,38]. HA–PLA PSs can achieve a high encapsulation efficiency (EE) and extend blood circulation time over that of PEG–PLA PSs [22]. Of course, most attractive for our purposes is the degradative behavior of HA and PLA. HA degrades in response to exposure to HYAL [39,40], as well as hexosaminidase A (HexA) [41], while HA [42] and PLA [43] both degrade in response to acidic environments. Of note, for diseases not associated with acidic environments, PLA is biodegradable even in neutral conditions, albeit at a delayed rate [44]. With the enzyme responsivity as the focus, our HA–PLA drug carrier will be relevant in any physiological pH conditions.

As highlighted in Figure 1, we created PSs from PLA and HA that can be delivered for HA block degradation by HYAL and pH hydrolysis (H⁺ ions) of the PLA polyester, leading to the release of therapeutic proteins in a highly pathology-driven approach. In this study, HA–PLA PSs were synthesized using a variety of HA MWs to optimize the size, surface charge, release behavior and biocompatibility of the PSs. Specifically, these HA–PLA PSs can be used for any disease associated with high HYAL or high β-hexosaminidase, as they serve biologically redundant purposes [41]. Furthermore, the general approach and methods can be used to guide the design of dual-responsive PSs for any disease that presents with upregulated enzymes. Highlighted below, we compare the performance of PSs made from 5-kDa, 7-kDa and 9-kDa HA with a consistent 15-kDa PLA block, with a specific focus on enzyme-responsive protein release.



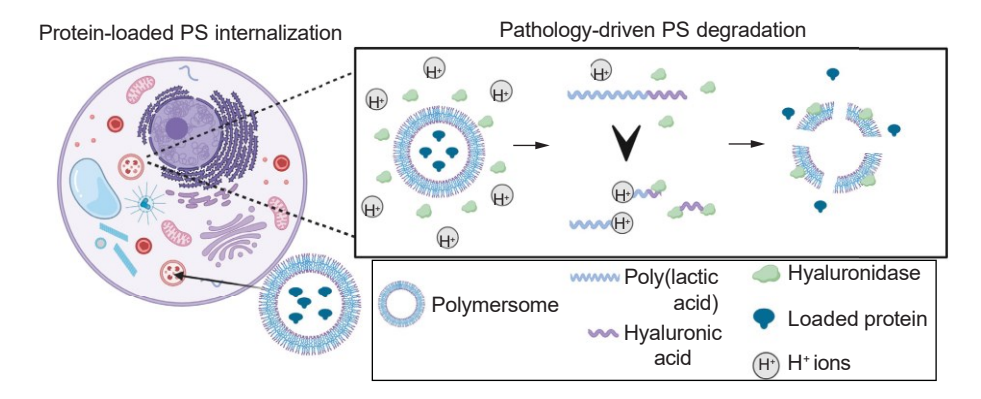


Figure 1. Representation of the pathology-driven approach for enzyme- and pH-responsive polymersomes. HA-PLA polymersomes will be delivered to the cellular lysosomes. Upon lysosomal entry, we anticipate observation of lysosome-localized enzymatic degradation of HA-PLA polymersomes in response to upregulated levels of HYAL (observed in various diseases) and therefore, lysosomal release of loaded protein. Simultaneously, as PLA is a polyester it will undergo hydrolytic cleavage by free H⁺ ions, leading to increased payload release. HA: Hyaluronic acid; HYAL: Hyaluronidase; PLA: Poly(b-lactic acid); PS: Polymersome.

Materials & methods

Materials

N-hydroxysuccinimide (NHS) activated PLA (PLA-NHS, MW 15 kDa) and HA (MW 5, 7 and 9 kDa) were purchased from Creative PEGworks (NC, USA). Polymers were chosen in accordance with the necessary hydrophilic fraction range for PS formation along with the goal of minimizing HA MW in order to maximize enzyme responsivity [35]. N,N-diisopropyl-ethylamine (DIPEA) and 1,4-diaminobutane were purchased from Acros Organics (Antwerp, Belgium). Sodium cyanoborohydride was purchased from Chem-Impex International (IL, USA). Slide-a-lyzer dialysis devices with a molecular weight cut-off (MWCO) of 3.5 kDa and 10 kDa (Spectrum Labs, CA, USA) were used in the polymer synthesis process. Float-a-lyzer dialysis devices (encapsulation studies) and slide-a-lyzers (release studies), both of MWCO 100 kDa, came from Thermo Fisher Scientific (MA, USA). DMSO was used in PS formation (Sigma Aldrich, MO, USA). Mannitol (Sigma Aldrich) at a concentration of 8 wt%/v was used as a lyoprotectant in all PS formation studies. Millex syringe filter units of pore sizes 0.45 µm (Millipore, MA, USA) were used when stated. Phosphotungstic acid (PTA) (Polysciences, Inc., PA, USA) was provided by the Clemson Electron Microscopy Facility for PS staining.

Fluorescein isothiocyanate (FITC)-tagged bovine serum albumin (BSA) and HYAL were purchased from Sigma Aldrich. PSs were concentrated using 100K microcentrifugal filters from Amicon Ultra (Millipore) preceding release studies. D Martin of Auburn University donated skin fibroblasts from GM1 gangliosidosis-affected cats (GM1SV3 cells) under a materials transfer agreement. GM1-affected cells were chosen as a model for these studies given that GM1 gangliosidosis pathology includes HexA upregulation [7,22], making a HYAL/HexA-responsive system especially relevant to this disease state. The medium was DMEM (Thermo Fisher Scientific) with 10% fetal bovine serum and 1× penicillin–streptomycin (Thermo Fisher Scientific). Passages were performed using 0.05% trypsin (Corning, Inc., NY, USA). Paraformaldehyde 16% solution (Electron Microscopy Sciences, PA, USA) and Vectashield with 4¹,6-diamidino-2-phenylindole (DAPI) (Vector Laboratories, CA, USA) were used for fixing and staining cells preceding microscopic imaging. Cytotoxicity was evaluated using a 3-(4,5-dimethylthiazol-2-yl)-5- (3-carboxymethoxyphenyl)-2-(4-sulfophenyl)-2H-tetrazolium (MTS) Cell Proliferation Assay kit from BioVision (CA, USA). All chemicals and reagents were of analytical grade.

Methods

Synthesis of HA–PLA block copolymers

HA–PLA was synthesized by an end-to-end coupling strategy, as described in previous research articles [22,45]. In short, the synthesis was performed as follows.

Amination of HA

HA was functionalized with a terminal amine group by a reductive amination reaction, allowing easy coupling to the terminal NHS group on the PLA. The reaction protocol is defined on a mass basis. In detail, 500 mg of



HA was dissolved in an 0.1 M acetate buffer (pH 5.4), then 0.5 ml of 1,4-diaminobutane was added dropwise into the HA solution under magnetic stirring. After 24 h of stirring at 50°C, 0.1 g of sodium cyanoborohydride (NaCNBH₃, 1.6 mmol) was added to the reaction mixture under stirring; the next day, 0.05 g of NaCNBH₃ (0.8 mmol) was added and stirred for another 24 h. The mixture was then dialyzed (MWCO 3.5 kDa) against type I deionized (MillQ) water for 72 h to remove excess 1,4-diaminobutane and NaCNBH₃ and obtain the purified amino-functionalized HA. Before lyophilizing, the polymer solution was filtered through a 0.45-µm syringe filter. Amination was confirmed via attenuated total reflection—Fourier transform infrared spectroscopy (ATR-FTIR) on a Perkin-Elmer (MA, USA) Spectrum Two FITR spectrometer.

Conjugation of HA-PLA

The conjugation reaction is defined on a molar basis. In a glove box under nitrogen gas, 0.3 g of PLA-NHS (0.02 mmol) was dissolved in DMSO. Then, 0.03 mmol of aminated HA, supplied at a 50% excess to PLA, was added to the DMSO along with 15 μl of DIPEA (0.091 mmol). After stirring at 50°C for 48 h, the mixture was dialyzed (MWCO 10 kDa) in type I deionized water for 72 h to remove excess HA and DIPEA; following dialysis, the solution was filtered by a 0.45-μm syringe filter. The final product, HA–PLA, was confirmed via ATR-FTIR spectroscopy and NMR on a Bruker Avance-300 NMR spectrophotometer (MA, USA). HA–PLA was finally lyophilized in preparation for PS formation.

PS formation

PS synthesis

HA–PLA PSs were formed using solvent injection. Briefly, HA–PLA was dissolved in DMSO at a concentration of 2.4 mg polymer/100 μ l DMSO. Using a syringe pump, the HA–PLA was injected into a solution of 8 wt%/v mannitol in type I deionized water at a rate of 20 μ l/min using a 21-gauge needle. The PS solution was then filtered through a 0.45- μ m syringe filter. PSs were lyophilized for further use; mannitol served as a lyoprotectant, as has been previously established in our lab for suitability in use with PSs of this type [22,46].

PS characterization

The particle size and ζ -potential of the HA–PLA PSs were determined via dynamic light scattering (Zetasizer Nano ZS90, Malvern Instruments, Malvern, UK). PS samples were suspended in deionized water for size measurements; the concentration required for consistent measurements was optimized individually for each PS formation (Supplementary Figure 1). To determine the surface charge, sodium chloride was dissolved in the undiluted PS solution to obtain a final salt concentration of 100 μ M prior to reading the ζ -potential. PSs were prepped for transmission electron microscopy (TEM) imaging at a concentration of 15 mg/ml before 1% phosphotungstic acid was applied for negative staining. TEM images were taken on a Hitachi 7830 UHR transmission electron microscope at 120 kV (Tokyo, Japan).

EE% of the FITC–BSA was evaluated on a mass basis as follows. FITC–BSA was dissolved in deionized water at a concentration of 2.2 mg/ml, then 10 μl of the FITC–BSA solution was vortexed with 10 mg of lyophilized PSs; 990 μl of deionized water was then added and mixed to obtain a total volume of 1 ml of the loaded PS solution. The loaded PSs were then added into a float-a-lyzer (MWCO 100 kDa) for dialysis against deionized water. Samples of the dialysate were taken over time to identify release of FITC–BSA over time. Each time a sample was taken, the buffer was changed to ensure that a concentration gradient was maintained and encourage complete diffusion of the released FITC–BSA into the dialysate [5]. The total FITC–BSA released into the buffer (C_r) was quantitatively analyzed by using UV-Vis spectroscopy (BioTek Synergy H1, Aligent Technologies; CA, USA); any FITC–BSA not released through dialysis was assumed to be encapsulated in the PSs. EE was calculated using the following equation:

$$EE(\%) = \frac{C_0 - C_r}{C_0}$$
 (Equation 1)

where C_0 is the original concentration of FITC–BSA added to the lyophilized PSs prior to dialysis and C_r is the measured concentration as back-calculated from the fluorescent signal.

Release studies

FITC-BSA loaded PSs were used for three different types of release studies, as represented in Figure 2. Initial release



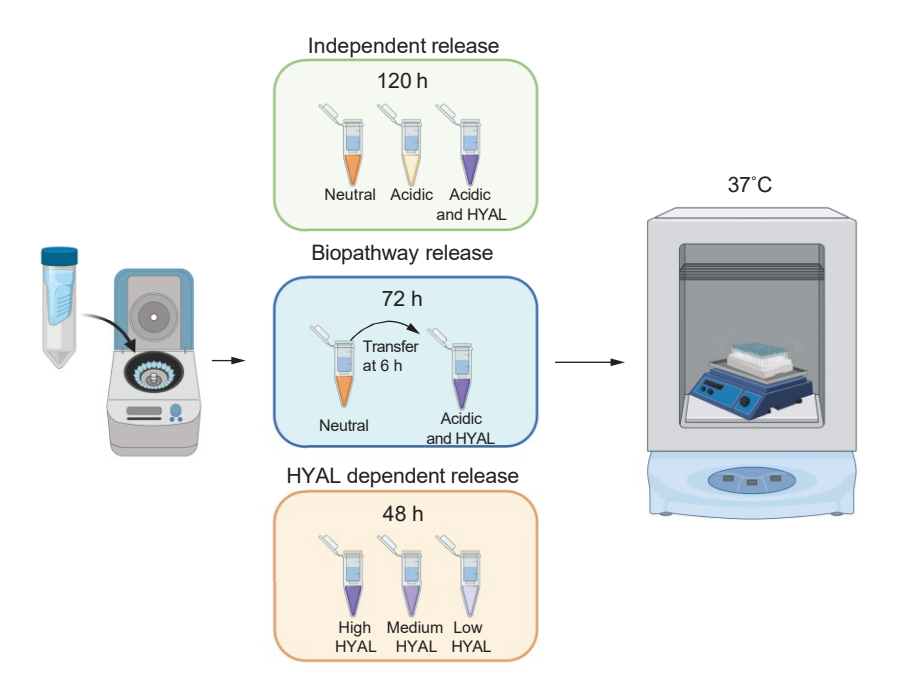


Figure 2. General release study setup and conditions. Loaded HA-PLA polymersomes were concentrated via centrifugal filtering and subsequently divided for dialysis in a variety of buffers. The independent release study examined FITC-BSA release in constant neutral, acidic, or acidic + enzymatic environments. The biopathway study observed release as a result of changing environment - specifically, the shift from neutral to acidic and enzymatic, as would be experienced upon internalization into the target pathological microenvironment. The HYAL-dependent release study examined release behavior in buffers with varied degrees of enzymatic activity. After loaded polymersomes were placed in respective buffers, the solutions were shaken and maintained at 37°C throughout the entirety of each study.

BSA: Bovine serum albumin; FITC: Fluorescein isothiocyanate; HA: Hyaluronic acid; HYAL: Hyaluronidase; PLA: Poly(b-lactic acid).

studies focused on a general comparison of release in different environments mimicking biological stimuli. First, 1 ml of concentrated PSs was divided into three mini slide-a-lyzers (MWCO 100 kDa) for dialysis against a 0.1-M HEPES buffer (pH 7.4), 0.1-M citrate buffer (pH 4.8), or 0.1-M citrate buffer (pH 4.8) with a concentration of 40 units/1 HYAL. The mini dialysis devices were exposed to 1.2 ml of buffer under constant shaking in an incubator maintained at 37°C to mimic physiological temperature. UV-Vis spectroscopy was used to evaluate FITC–BSA release into the various buffers over the course of 5 days; fresh buffer was provided at each sample time. The second study was intended to model the biological pathway, where PSs would first travel through the buffered blood solution (pH 7.4) before entering a cell and an acidic lysosome with upregulated enzyme activities (pH 4.8 and HYAL), by examining the release from successive exposure to relevant environments. In this study, PSs were suspended in 100 µl of neutral buffer (pH 7.4 and no HYAL) and were dialyzed against this buffer for the first 6 h. The dialysis devices were then transferred into the acidic, enzymatic buffer (pH 4.8 + HYAL) where release behavior was observed through UV-Vis spectroscopy for the remainder of the 48-h study period.

In vitro studies

Immortalized feline fibroblasts isolated from GM1-affected felines (GM1SV3 cells) were seeded for each cell study at densities given in Supplementary Table 1; treatment was given according to cell density at a ratio of 100 µl concentrated PSs per 5 × 10⁶ cells. Cells were seeded separately for 4-h and 24-h treatments and allowed to attach overnight preceding treatment. Following washing, cells were treated with a combination of concentrated PSs and fresh media at set concentrations; cells were incubated at 37°C and under 5% CO₂ for the entirety of the corresponding treatment window.



Microscopic imaging

After treatment, cells were rinsed with phosphate-buffered saline; paraformaldehyde (PFA) solution (diluted to 4%) was then added and allowed to sit for 10 min. The rinsing and fixing steps were repeated a total of three times. Then, DAPI was applied to the fixed cells. The cells were imaged for FITC and DAPI fluorescent signals on an Echo Revolve (Echo, CA, USA) and an image overlay was performed.

Flow cytometry

Cells were collected from wells via trypsin, resuspended in phosphate-buffered saline and kept on ice awaiting analysis. Flow cytometry was performed using a Cytek Aurora (CA, USA). Signal gating was based on the B2 channel and limits were set according to untreated control cells; an example is provided in Supplementary Figure 2.

Cytotoxicity

Cytotoxicity was evaluated using an MTS assay. At the end of the treatment period, MTS reagent was added to the medium at 10% by volume of the total working volume of the well. The cells were incubated for another 4 h before absorbance readings were taken at 490 nm on a UV-Vis BioTek Synergy H1. Cell viability was quantified as a ratio of the absorbance of the treated cells to the absorbance of untreated control cells.

Statistical analysis

EE data were analyzed using both a one-way Brown–Forsythe and a Welch analysis of variance test with an α of 0.05. All release study data were analyzed using unpaired *t*-tests with Welch's correction with an α of 0.05. The difference in uptake of flow cytometry and viability via MTS from 4 to 24 h was confirmed using an unpaired *t*-test with an α of 0.05. In all cases, outliers were removed prior to determining statistical significance using a Grubbs test

Results

HA-PLA polymer conjugation

ATR-FTIR spectroscopy was performed on PLA-NHS, on HA (before and after amination) and on HA-PLA following polymer conjugation. Supplementary Figure 2 shows the respective FTIR spectra of all HA-PLA copoly- mers and corresponding intermediate polymers. FTIR on PLA-NHS revealed characteristic absorption bands at 1756.45, 1182.49 and 1088.64 cm-1 which are attributed to the -C=O and -C-O stretching characteristic of ester groups. Additionally, a weak signal at 2999.5 cm⁻¹ was representative of -C-H stretching. The broad stretch at 3289 cm⁻¹ on the FTIR spectrum of HA was attributed to hydroxyl groups, while sharp peaks around 1737.3, 1609.88 and 1151 cm⁻¹ and 1040.70 cm⁻¹ corresponded to C=O (carbonyl) and C-O (ether) stretching, respec- tively. As compared with the HA spectrum, the aminated HA spectrum exhibits a broadening to bands appearing around 3273.81 and 1597.56 cm⁻¹, both of which are associated with -N-H vibration types. The HA-PLA spectrum showed characteristic peaks from both PLA-NHS (the sharp 1764.40 cm⁻¹ peak) and HA (peaks at 3283.66, 1601.40 and 1041.28 cm⁻¹), which indicates that the polymer conjugation was completed successfully. Broadening of the characteristic peaks of HA, which overlap with various peaks of PLA-NHS, further support successful coupling. NMR of the final polymer further supports the polymer conjugation based on comparison with individual HA and PLA-NHS spectra (Supplementary Figure 3). Namely, two additional peaks, around 1.5 and 2.9 p.p.m., can be observed in HA-PLA when compared with HA; those peaks correspond nicely with the characteristic peaks of PLA-NHS.

PS formation & characterization

Dynamic light scattering was used to determine hydrodynamic diameter (HD) as well as polydispersity index (PDI) and ζ -potential of HA–PLA PSs formed using 5-, 7- and 9-kDa HA blocks while maintaining a PLA block of 15 kDa (Table 1). There was no discernible trend associated with changes in HA MW and PS diameter, PDI or ζ -potential as demonstrated by the lack of statistical significance between any values. TEM images were taken of each PS formulation (Figure 3) and confirmed the formation of spherical PSs with relatively monodisperse size distributions.

FITC-BSA, a hydrophilic protein, was chosen to model the protein-loading capacity for each PS system. Loading of FITC-BSA ranged from around 9 to around 7 µg of protein per 10 mg of PSs, as shown in Table 1, with the average EE decreasing slightly with increasing MW. Despite the clear trend, all EE values were statistically the same regardless of the change in HA MW.



Table 1. Physical characterizations of polymersomes.			
	HA(5 kDa)-PLA	HA(7 kDa)-PLA	HA(9 kDa)-PLA
f	0.25	0.32	0.38
HD (nm)	82.0 ± 10.2	76.5 ± 7.7	99.6 ± 3.1
PDI	0.40 ± 0.05	0.45 ± 0.03	0.26 ± 0.01
z-potential (mV)	-24.9 ± 2.8	-29.6 ± 2.7	-25.5 ± 3.5
EE (%)	45.56 ± 13.06	40.71 ± 9.11	34.54 ± 10.26
Drug loaded (μg/10 mg)	9.11 ± 2.61	8.14 ± 1.82	6.91 ± 2.05

The examined polymersome formulation can be differentiated firstly by hydrophilic fraction as given by f. Physical characteristics (HD, PDI and z-potential) of each resulting polymersome system were determined immediately following synthesis by dynamic light scattering. EE studies were performed on lyophilized polymersomes using FITC-BSA in a dialysis procedure. Drug loading is the total mass of FITC-BSA assumed to be loaded into the polymersomes per dry polymersome mass. Values are given as means ± standard deviation as calculated from a dataset of n = 5. Student's t-tests comparing each EE value for one set of polymersomes to one of the other two formulations showed no statistical difference between any set.

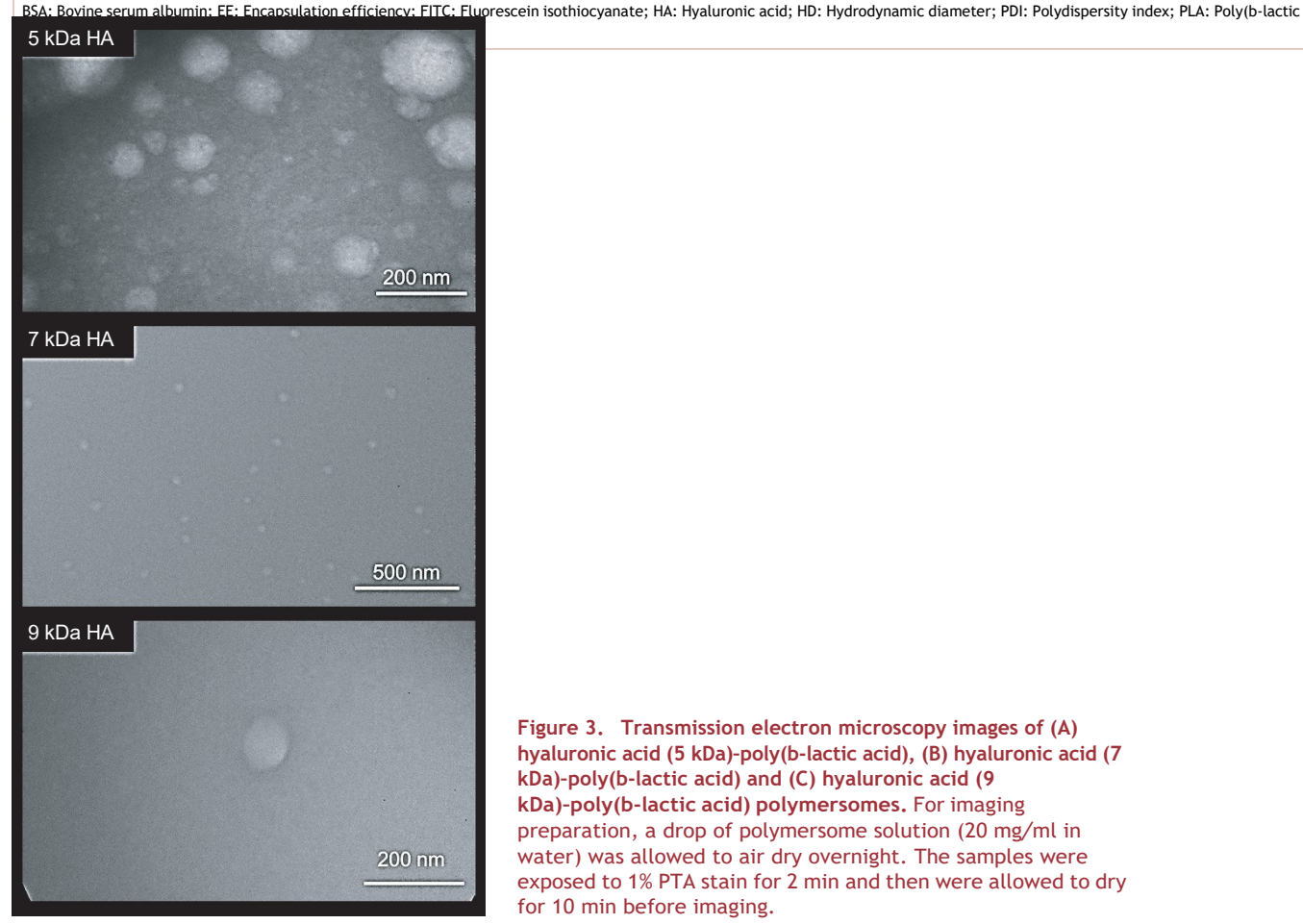
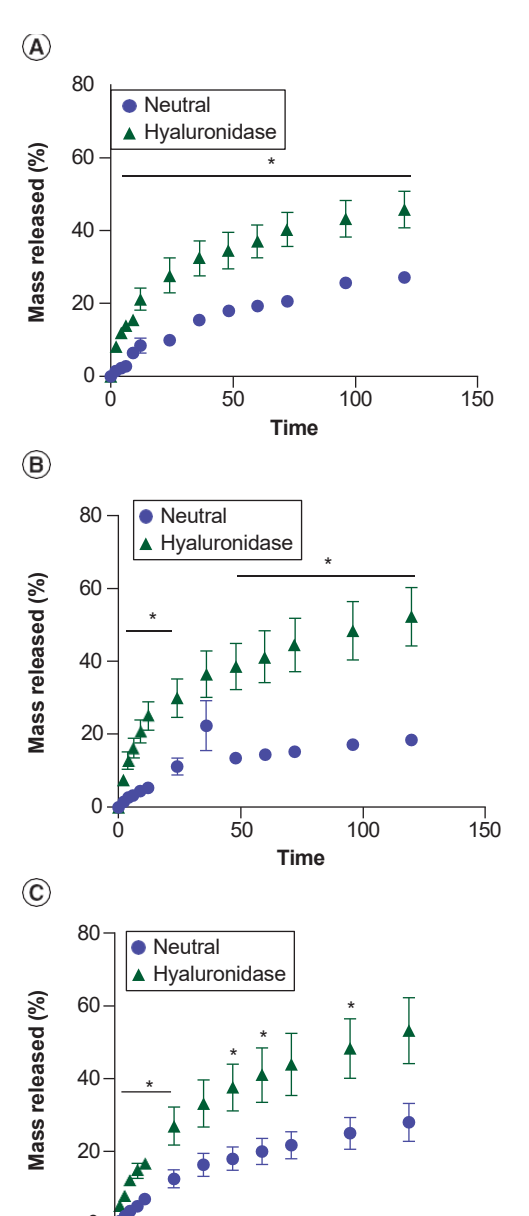


Figure 3. Transmission electron microscopy images of (A) hyaluronic acid (5 kDa)-poly(b-lactic acid), (B) hyaluronic acid (7 kDa)-poly(b-lactic acid) and (C) hyaluronic acid (9 kDa)-poly(b-lactic acid) polymersomes. For imaging preparation, a drop of polymersome solution (20 mg/ml in water) was allowed to air dry overnight. The samples were exposed to 1% PTA stain for 2 min and then were allowed to dry for 10 min before imaging.

Release of the protein payload was evaluated in three buffers modeling relevant release environments (Figure 4). In the bloodstream, the environment is neutral with a pH of around 7.4, which is modeled by the HEPES buffer. Acidic destinations, like that of the lysosome or tumor, are modeled by citrate buffer of pH 4.8. The target disease microenvironment in total is modeled by a citrate buffer concentrated with 40 units/l of HYAL. HYAL resides primarily in the lysosome, so we chose to model HYAL upregulation as an increase to normal lysosomal levels. In a healthy lysosome, HYAL is typically at a concentration of around 11 units/1 [47]. Using GM1 gangliosidosis, a neuropathic lysosomal storage disorder, as a reference, a diseased lysosome has a concentration of HA-degrading enzymes about 3.7-times greater (around 40 units/l) [22]. FITC-BSA release into each buffer was monitored over the course of 120 h. The release behavior in the acidic buffer was not found to be statistically different throughout





50

Time

100

150

Figure 4. General release profiles of fluorescein isothiocyanatebovine serum albumin from (A) hvaluronic acid (5 kDa)-polv(blactic acid), (B) hyaluronic acid (7 kDa)-poly(b-lactic acid) and (C) hyaluronic acid (9 kDa)-poly(b-lactic acid) polymersomes. Polymersomes previously loaded and dialyzed as outlined for EE studies were concentrated for release studies in constant buffer environments over the period of 5 days. Equal polymersome volumes were added to microdialysis devices that were suspended in neutral or enzymatic/acidic buffers for the full course of the study. Fresh buffer was provided at each sample time point; the devices were constantly shaken and kept at 37°C. Study was repeated for n = 5. Quartile tests were performed to identify outlier points; those points were disincluded from statistical analysis. The remaining data were analyzed via Student's t-test to identify statistical difference between release profiles. *p < 0.05; **p < 0.005; ***p < 0.0005. BSA: Bovine serum albumin; EE: Encapsulation efficiency; FITC: Fluorescein isothiocyanate; HA: Hyaluronic acid; PLA: Poly(b-lactic

the full study in comparison to either the neutral or HYAL buffers (Supplementary Figure 4). FITC–BSA release was greater in the enzymatic buffer than in the neutral buffer for each PS formulation regardless of HA block MW. The final percentages of FITC–BSA released following incubation with HYAL were 54.1 ± 11.0, 47.7 ± 18.3 and 46.7 ± 20.1% for HA(5 kDa)–PLA, HA(7 kDa)–PLA and HA(9 kDa)–PLA, respectively. The second release study examined the release behavior of a non-constant environment – modeling the release in response to the biological pathway of intravenously injected PSs. Specifically, the PSs would spend time in a neutral environment (the blood) before ever being internalized to the target lysosomes. Based on data obtained on the characterization properties and performance of PSs in the release study performed under independent conditions, the biologically relevant release study was only performed with the HA(5 kDa)–PLA and HA(7 kDa)–PLA (Figure 5). Both PS formulations presented with minimal release over the first 6 h while they were kept in neutral solution. After the 6-h incubation mimicking transport through the bloodstream, the PSs were placed in a buffer with both pH and enzymatic stimuli, mimicking localization to the pathological area. A burst release was observed once they were transferred into the lysosome-like environment, after which FITC–BSA release was Fickian for the rest of the study.

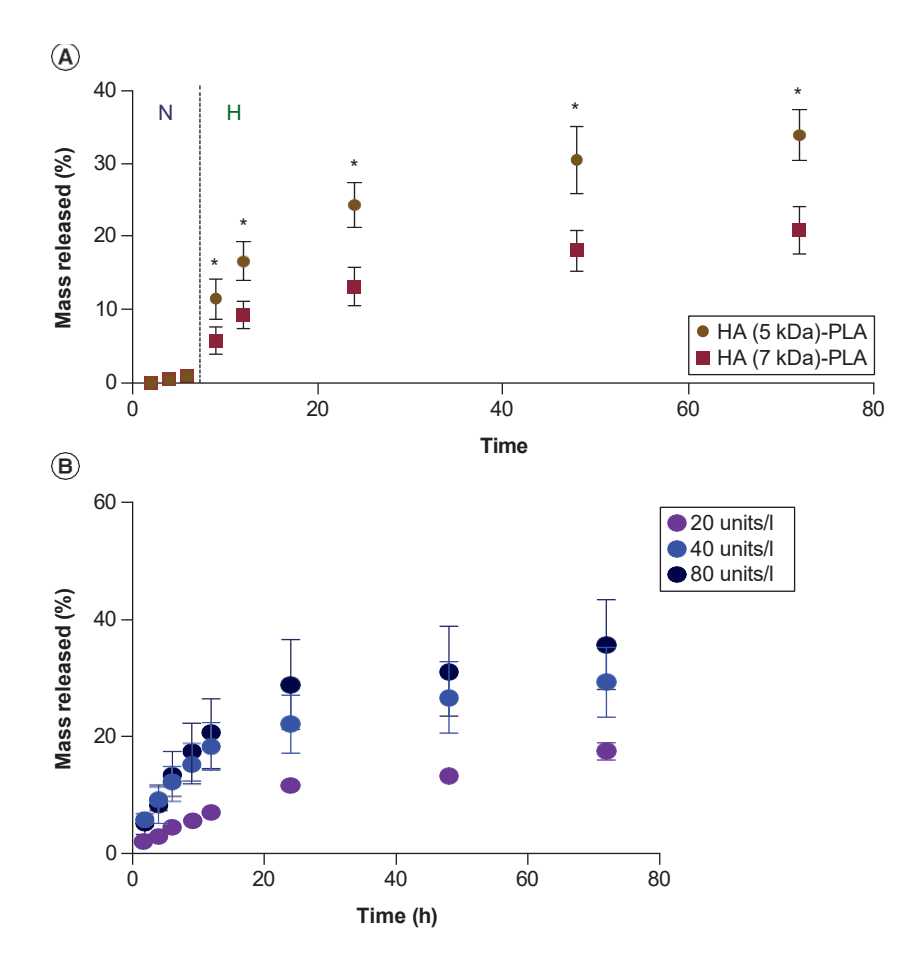


Figure 5. Specialized release profiles of fluorescein isothiocyanate-bovine serum albumin. (A) Biopathway release HA(5 kDa)-PLA and HA(7 kDa)-PLA polymersomes. (B) HYAL-dependent release HA(5 kDa)-PLA polymersomes. Polymersomes previously loaded and dialyzed as outlined for EE studies were concentrated for release studies designed (A) to model the environmental conditions following intravenous administration or (B) to examine differences in polymer degradation behavior as driven by enzyme activity. Equal polymersome volumes were added to microdialysis devices that were suspended in neutral buffer for the first 6 h; after 6 h, the devices were moved into and maintained in enzymatic/acidic buffer for the remainder of the study. Fresh buffer was provided at each sample time point; the devices were constantly shaken and kept at 37°C. Study was repeated for n = 3. Data were analyzed via Student's t-test to identify statistical difference between release profiles.

BSA: Bovine serum albumin; EE: Encapsulation efficiency; FITC: Fluorescein isothiocyanate; HA: Hyaluronic acid; HYAL: Hyaluronidase; PLA: Poly(b-lactic acid).

The final release study, assessing the dependence of polymer degradation and hence drug release on enzymatic activity, was performed only on the HA(5 kDa)–PLA PSs (Figure 5). Rates of polymeric degradation appeared to correlate positively with increases in HYAL concentration, with a greater percentage drug release observed at higher enzyme concentrations.

As we are experts in GM1 gangliosidosis [5,22,48] and it presents with upregulated β -hexosaminidase, we chose to use it as a model for our PS performance. Cellular internalization of a single, uniform dose of FITC–BSA-loaded PSs by GM1 gangliosidosis-affected feline fibroblasts, GM1SV3 cells, was analyzed at 4 and 24 h after treatment by fluorescence microscopy and flow cytometry. Untreated GM1SV3 cells were used as a control. The untreated cells demonstrated a lack of FITC fluorescence, while all treated cells showed clear green fluorescence, indicating cellular uptake of the HA–PLA PSs (Figure 6). Flow cytometry confirmed cellular internalization of the FITC–BSA in the cells treated by each PS formulation (Supplementary Figure 6). The FITC fluorescent signal was clearly higher in the 24-h-treated cells than after 4-h-treated cells with all PS formulations. Each PS formulation enabled cellular uptake in over 90% of single cells at 4 h. Cellular uptake at 24 h was less consistent, with the population of cells maintaining FITC fluorescence 24 h after treatment decreasing with HA(7 kDa)–PLA and HA(9 kDa)–PLA



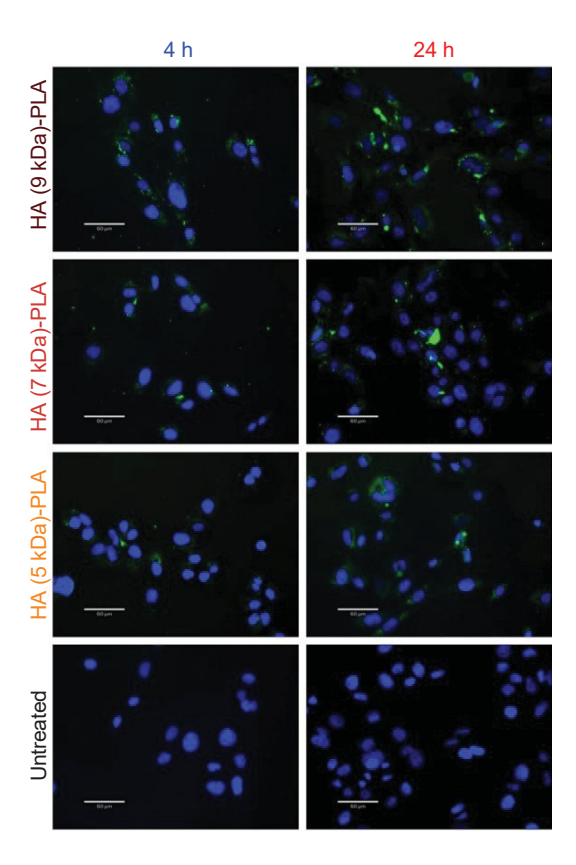


Figure 6. Fluorescent microscopy images of cellular uptake following treatment with fluorescein isothiocyanate-bovine serum albumin-loaded polymersomes. GM1SV3 cells were incubated with a mixture of fresh media and concentrated polymersomes (previously loaded and dialyzed) for 4 or 24 h. At completion of the treatment window, the cells were rinsed then stained three times with DAPI. Cells were finally fixed and allowed to dry overnight before imaging. Untreated cells (cells incubated in only media) were used as a negative control. Green fluorescence shows the presence of FITC while blue fluorescence indicates nuclei based on DNA content. Separate images using the appropriate laser for each stain were taken and overlaid. In all treated cells, FITC can be observed to surround the nuclei, suggesting cellular localization throughout the cell as would be expected for lysosome internalization. DAPI: 4¹,6-diamidino-2-phenylindole; FITC: Fluorescein

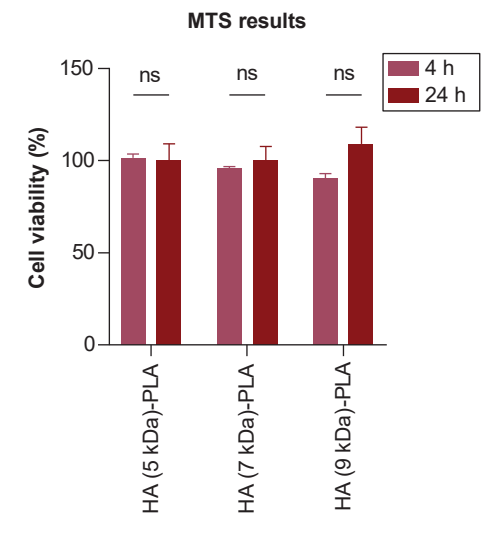


Figure 7. Yield of the colorimetric method for accessing cell viability. Cells were incubated with concentrated polymersomes and fresh medium for 4 or 24 h, or in only medium for the negative control, after which the MTS reagent was added at 10% of the total volume of the well. Cells were further incubated for 4 h, then absorbance measurements were taken. Results for treated wells were normalized against absorbance values of the control to give cell viability as a percentage. These tests were repeated for an n = 3. No statistical difference was found between treatment groups or time points when compared by Student's *t*-test. MTS: 3-(4,5-dimethylthiazol-2-yl)-5-(3-carboxymethoxyphenyl)-2-(4-sulfophenyl)-2H-tetrazolium; ns: No significance.

PSs, although the decrease was not statistically significant. However, the HA(5 kDa)–PLA PSs showed a clear and statistically significant increase in uptake at the 24-h time point.

isothiocyanate.

Finally, cell viability at a constant treatment concentration of 100 μ l concentrated PSs per 5 × 106 cells was shown to be high for all formulations at both time points (Figure 7); in fact, at 24 h each formulation exhibited cell viabilities around 100%, suggesting that the PSs are highly biocompatible and do not impact the cellular environment in the long term.

Discussion

Success of both polymer reactions (amination and conjugation) was confirmed via ATR-FTIR spectroscopy (Supplementary Figure 2) and NMR (Supplementary Figure 3). The absence of the alkyne signal in the aminated HA spectra confirms amination of HA. The HA–PLA spectrum showed characteristic peaks from both individual



polymer (PLA-NHS and HA) spectra and exhibited a general broadening to peaks that were similar or overlapping in the individual spectra, which indicates that the polymer conjugation was carried out successfully. In the NMR spectra, characteristic peaks from both HA and PLA-NHS are clearly present in the HA–PLA spectra, indicating successful copolymer formation.

Each polymer formulation led to PSs with diameters around or less than 100 nm, although statistically the formulations do not differ based on size. HA is known to have higher cohesivity in solution with higher MW, meaning that heavier polymers are more prone to aggregate and self-entangle to minimize the thermodynamic energy that results from aqueous interactions [35]. Accordingly, PS size was expected to decrease with increasing MW due to tighter polymer packing around the core. The HA(9 kDa)-PLA PSs behave differently, however. This suggests that polymer cohesivity is not the only factor at play in determining PS size. Possible explanations for a larger diameter with higher HA MW could include increased membrane thickness (which increases with polymer MW [7,49]) or incidence of unbound polymer. Given that HA is a linear polymer, increasing MW means a longer polymer length, so any unbound polymer ends may, too, be longer, giving the appearance of a greater HD. The relatively high PDI of each polymer formulation is reasonable for a system of this nature. PSs are self-assembled so they are prone to wide particle size distribution in general [50-52]. Adding to that, biopolymers like HA exhibit inherent variability and complexity over synthetic alternatives, which could affect the thermodynamics of assembly and subsequent morphology of the final system [53]. Finally, each PS also had a negative ζ -potential in the midto-high twenties, which is desirable for nanoparticle stability as well as beneficial for lysosome internalization [54], which would be useful for reaching the highest concentrations of HYAL, especially for designs for lysosomal storage disorders.

The EE values of the PSs in this study are reasonable when compared with examples in the literature that use the same loading protein and loading protocol, assuming that EE is an approximately linear function of PS size. Direct comparisons of similar PSs and their protein-loading capacity showed decreasing EE with a decreasing PS diameter [22]. We hypothesize that the reason for decreased loading with increased MW is that the heavier polymers create a smaller inner cavity due to the additional length of the unbound polymer ends, which bulk up and fold into the interior space. After attributing the increased PS diameter to more unbound polymer ends on the exterior of the PS, it follows that the unbound polymer ends would also take up significant interior core volume, given the bilayer makeup of the PS membrane, and decrease the space available for high-MW protein loading. Additionally, the higher cohesivity levels in higher-MW HA [35] may draw the polymer membrane in more tightly, decreasing cavity space. Previous work by our lab demonstrated that HA(15 kDa)-PLA(25 kDa) PSs with diameters of 138.0 ± 17.6 nm achieved a FITC-BSA EE of 77.7 ± 3.4% [22]. Although the EE was notably larger in this study, so too was the HA MW, and therefore the resulting PS diameter and interior volume. Comparing the PSs made from HA(5 kDa)-PLA PSs, for example, with our previous work [22], it can be seen that both diameter and EE decreased by the same factor (about 59%). Furthermore, this trend appears to be material-independent, with similar proportional decreases between EE and diameter being observed in a study on PEG-PLA PSs, which tend to serve as the gold standard for PSs in drug delivery. Kelly et al. cited EE of 72 ± 12% for PSs of a 145 ± 21 nm diameter [5], which is very similar to the size and EE observed in our previous study [22] and therefore also scales proportionally to our PS formulations. HA(9 kDa)–PLA PSs were an outlier to the observed trend. Despite having the largest diameter of the formulations in this study, HA(9 kDa)-PLA PSs exhibited the lowest EE. This is likely attributed to a lower core volume; membrane thickness in a PS increases with increasing polymer MW. Therefore the HA(9 kDa)-PLA should be expected to have the thickest membrane, which will constrict the empty interior space. Additionally, the unbound polymer lengths that have been already mentioned as possible factors increasing the overall PS diameter can also be expected to appear at the core interface, further restricting loadable core volume, due to the bilayer nature of the membrane. Considering the larger diameter, which is less helpful for size-dependent brain transport, and the low loading capacity of the HA(9 kDa)-PLA PSs, this formulation presented as the least promising option at this stage. In contrast, the HA(7 kDa)-PLA block copolymer led to PSs that were the most consistent and reproducible, demonstrated by low standard deviation values for the HD as well as EE.

In the independent release study, the final percentage of FITC–BSA released over 120 h decreased with increasing HA MW. This trend is expected based on other reports. Namely, high-MW HA is less susceptible to enzymatic degradation [35]. It has also been noted in different types of polymeric nanomaterials that degradation is more pronounced in copolymers of lower HA fraction and polymers with lower cohesivity [39,55]. pH-driven HA degradation has not been shown to correlate in any way with MW [35], so although it does certainly contribute to the overall degradation profile of each PS, it is not thought to contribute to the variability between PS systems.



Pairing the decreasing trend for EE and final release percentage, the HA(5 kDa)–PLA PSs delivered the greatest total drug payload over the course of the study. It is worth noting that the independent release study was ended before a definitive plateau was observed for any formulation, so it is feasible that a greater final release percentage would be achieved at final steady state. Regardless, the results support these PSs for use as sustained-delivery agents for a period of at least 5 days. This is beneficial toward decreased frequency of administration for PSs in general as a treatment which must be repeatedly administered, due to the frequent genetic nature of protein deficiency-related conditions. Sustained release is likely related to the dual enzyme- and pH-responsive nature of the PSs, with lower-MW HA-based formulations experiencing the greatest enzyme responsivity, as previously stated. However, a large PDI may also contribute to sustained release. Staggered degradation could therefore be further tuned or extended through a mixture of PSs made of different-MW HAs which would degrade in different amounts of time to for payload release.

In all formulations, exposure to HYAL increased drug release when compared with the neutral buffer. This confirms that PS degradation would be triggered by internalization into the pathological environment and that each PS would be suitable for targeted drug delivery for LSDs. Both HA(5 kDa)-PLA and HA(7 kDa)-PLA PSs trended toward significantly increased release in the enzymatic buffer over the acidic buffer. The dependence of payload release on HYAL was further examined as a function of HYAL concentration in the final release study, where we chose to examine only the HA(5 kDa)-PLA PSs on account of the larger enzymebased response observed in the biopathway release study as compared with HA(7 kDa)-PLA. On average, the payload release at each given time point was trending toward significantly increasing with increasing HYAL concentration, especially with the increase from 20 to 40 units/l. In no case, however, was release statistically different between buffers with different HYAL activities in the concentration ranges examined here. The results of this study are significant to note when comparing these PS formulations with publications for HA-PLA PSs 122] as well as HA-based micelles [56] and nanocapsules [38], wherein responsiveness to HYAL incubation was previously noted. Specifically, a twofold increase in payload release was noted in both the PSs and micelle systems (loaded with FITC-BSA and doxorubicin, respectively), after HYAL incubation versus incubation in a simple acidic buffer [22]. Both of the aforementioned studies used much higher HYAL concentrations in solution. Enzymes are characterized on a unit basis to quantify enzyme activity, which does not correspond directly to mass when compared batch to batch [57]. Suppliers for the materials cited in these papers guarantee 300 units/mg or above [58]; therefore, concentrations of 1–2 mg/ml result in a solution concentrated to at least 300,000 units/1 of HYAL. Our studies focused on HYAL concentrations of only 40 units/l, a more biologically relevant value, but also examined additional concentrations for comparison to develop a stronger understanding of how enzymedriven degradation can change with changing enzyme concentration. Enzyme-driven degradation was shown to be directly proportional to enzyme concentration, albeit not significantly on this scale, so it is not a surprise that we would see less of a response in our study when comparing acidic buffers with and without enzyme. Nonetheless, this is promising for patient-specific treatment, as we should be able to expect to see greater release differences in regions or patients with further elevated HYAL (or HexA) levels, indicating a worse disease state. HA(5 kDa)-PLA and HA(7 kDa)-PLA PSs may, then, have promise for developing patient-specific treatment courses. The HA(9 kDa)-PLA formulation deviated from the expected trend, with acidic release being greater than release in enzymatic solution after 48 h. This may be attributable to the aforementioned decreased enzymatic degradative response that is observed in heavier HA polymers.

The biologically relevant release study further supported the joint pH- and enzyme-responsiveness of our PSs, as well as showing that these PSs can protect most of their payload until they have been localized to the target environment. In the acidic, enzymatic environment, the HA(5 kDa)–PLA PSs showed a more pronounced release than the HA(7 kDa)–PLA PSs. This is explained by the increased enzymatic degradation responsiveness of lower- MW HA and suggests that the use of a lower-MW HA polymer in lysosome-aimed PS applications might be the most conducive to fast, targeted release. However, this increased release must be weighed against the potential for sustained release. A sharper burst release may decrease the drug payload that can be continually released after initial lysosome internalization.

Fluorescence microscopy indicated an increased FITC–BSA presence at 24 versus 4 h (Figure 6), suggesting that cellular uptake is time-dependent. However, flow cytometry did not further confirm this trend (Supplementary Figure 6). Interestingly, as HA MW increases, the population of cells without FITC–BSA, as measured by flow cytometry, increases at 24 h, in contradiction with fluorescent images. Statistically, however, the 4- and 24-h time points were not different for the heavier HA(7 kDa) and HA(9 kDa) PS formulations, as determined by flow cytometry. It is not likely that PS expulsion is occurring with extended treatment times, but it can also not be



confidently said, for any but the HA(5 kDa)–PLA PS formulation, that uptake increases with treatment time. Therefore, the conclusion that can be made most confidently from the flow cytometry results is only that the HA(7 kDa)–PLA and HA(9 kDa)–PLA PSs behave less consistently when it comes to uptake than the HA(5 kDa)–PLA PSs. Nonetheless, these results are generally parallel to the fluorescence microscopy images and indicate that each formulation was effectively endocytosed by GM1SV3 cells. The cellular uptake achieved for each formulation at either time point was comparable to the 93.3 ± 3.6% uptake measured by in our previous work for the HA–PLA PSs [22], validating these results. HA-based PSs may have a natural advantage for facilitating uptake compared with PEG-based alternatives. A PEG brush on the exterior of PSs can reduce direct cell–carrier interactions with cells and hence uptake, which is why PEG is good at facilitating increased circulation times *in vivo* [59]. HA lacks this brush and is a receptor recognized by relevant cells.

GM1SV3 viability was statistically the same at both 4 and 24 h (Figure 7). However, viability may be slightly lower at 4 h postincubation. A possible explanation for this is that the generation of free, small-chain HA in the degradation process had a more acute effect, inducing pH changes to the cell media solution at earlier time points following the burst release. At longer time points, the in vitro microenvironment has had more time to equilibrate and is not experiencing an appreciable difference from the normally neutral pH, as evidenced by pH indicators (Supplementary Figure 5). Therefore, this does not present as a significant cytotoxicity concern, especially given that the reduction of in vitro viability at 4 h does not cross the biocompatibility threshold of 80% [60]. At the 4-h time point only, although cell viability is still consistently high, there is a potential decrease in cell viability with increasing MW. It is well known that HA is involved in the inflammation process and furthermore that HA MW dictates the body's physiological response [33]. All HA used in this study is low-MW HA (1000 kDa or lower), which means it is proinflammatory, such that treated cells may experience a slight inflammatory response which could contribute to decreased cell viability. The decreasing trend can then be explained as a function of HA MW and degradation products. Higher-MW HA has a longer chain as compared with lower-MW counterparts and has the most opportunity to generate small HA fragments. In the context of this study, then, HA(9 kDa)-PLA PSs would generate the most HA fragments, followed by HA(7 kDa)-PLA and HA(5 kDa)-PLA, respectively. The recovery of cell viability to nearly 100% at 24 h speaks to the quick resolution of the potential inflammatory process. Such low levels of cytotoxicity fit with the expectations for this study, as HA is largely cited as biocompatible and nontoxic in a variety of drug-delivery and nanoparticle applications [61-64].

Conclusion

The PSs examined here all exhibited properties and performances that made them attractive for applications as a drug carrier for protein-based therapy. It is important to note that selecting a MW of HA for HA-PLA PSs for protein-based therapy will be application-dependent, as properties were different between formulations. In general, PS size was seen to be a function of the cohesivity and length of the polymer chains, which are both related to MW. The sub-100-nm PS size of each formulation is promising toward facile cellular entry, especially as paired with negative ζ-potential [65]. EE decreased with MW, although not significantly, but was maintained at relatively high levels. Sustained release was achieved in all PSs over 5 days, with all formulations exhibiting similar release behavior. HA(7 kDa)-PLA PSs exhibited the greatest difference between release when in neutral buffer versus pathological conditions. Environmental responsiveness was seen in enzyme-rich and acidic environments, supporting any PS formulation for triggered-release applications. HYAL-driven polymer degradation was significant at the lowest doses explored and increased with increasing HYAL concentration. All PSs entered GM1affected cells (GM1SV3) at a high efficiency after 4 and 24 h with limited to no viability concerns. Based on low protein loading and enzyme responsivity, the HA(9 kDa)-PLA PSs showed the least desirable average makeup and performance as an enzyme- and pH-responsive protein-delivery vehicle. As for the other two formulations, both have merits that must be weighed against the desired application, specifically dependent upon the disease of interest. In terms of physical properties and cytotoxicity, the HA(7 kDa)-PLA PSs showed more uniformity than HA(5 kDa)-PLA PSs, although the two were not statistically different. In terms of the release study results, the HA(5 kDa)-PLA PSs exhibited more uniform release profiles, which suggests that it would be more controlled, but the HA(7 kDa)-PLA PSs showed more promise for sustaining release or differentiating release based on disease severity. Differentiating these PSs is difficult as their properties are similar, but even the minute details could result in different pharmacokinetic strengths in a clinical setting. In conclusion, HA(5 kDa)-PLA and HA(7 kDa)-PLA PSs are both attractive for applications as protein-delivery vehicles, and the choice of formulation will depend on what is considered most valuable to a drug system's performance. HA(5 kDa)-PLA PSs experienced the greatest burst release upon placement



Research Article Foster, Cakley & Larsen

in a pathological buffer after being exposed to a neutral buffer, which leads us to believe that this formulation may be better at payload protection during delivery. The responsive release behavior of these PSs was seen to trend toward HYAL concentration dependence, which further confirms their potential relevance in patient-specific, personalized treatment development; additionally, release behavior could be further strengthened by targeted drug-delivery strategies, specifically by ligand modification for enhanced targeting. These PSs could certainly be developed as drug carriers for use in a variety of diseases and conditions.

Summary points

- Biological barriers make protein-based therapies challenging to deliver efficiently.
- Polymersomes are self-assembled polymeric vesicles capable of encapsulating hydrophobic and hydrophilic drugs, proteins included.
- Polymersomes can be made to be responsive to pathology-related stimuli, like enzyme upregulation and changing pH.
- Hyaluronic acid is degradable by certain enzymes and in acidic conditions when integrated into polymersomes.
- Polymersomes assembled from hyaluronic acid (HA) and poly(b-lactic acid) (PLA) experienced responsive release through both pH- and hyaluronidase-triggered degradation.
- All formulations explored- HA(5, 7, or 9 kDa)-PLA(15 kDa) led to polymersomes with small sizes and moderate loading capacities.
- Molecular weight impacted polymersome properties, including diameter and encapsulation efficiency, and stimuli-responsive release behaviors, although not always to a statistically significant degree.
- Both HA(5 kDa)-PLA and HA(7 kDa)-PLA formulations exhibited clinically translatable strengths.

Supplementary data

To view the supplementary data that accompany this paper please visit the journal website at: www.futuremedicine.com/doi/suppl/10.2217/nnm-2023-0300

Author contributions

D Foster and J Larsen were responsible for the conception and design of experiments, analysis and interpretation of the data and revising this work critically for intellectual content. D Foster was responsible for conducting experiments and drafting of the paper; A Cakley assisted in conducting experiments. All authors approved the final version to be published; and agree to be accountable for all aspects of the work.

Acknowledgments

The authors thank D Martin and A Gross at Auburn University for the use of the GM1SV3 cell lines and E Davis for the use of ATR-FTIR spectrophotometer.

Financial disclosure

This work was supported in part by the National Science Foundation CAREER program under NSF Award no. 2047697. Support was also received from Clemson University's Creative Inquiry program. The authors have no other relevant affiliations or financial involvement with any organization or entity with a financial interest in or financial conflict with the subject matter or materials discussed in the manuscript apart from those disclosed. This includes employment, consultancies, honoraria, stock ownership or options, expert testimony, grants or patents received or pending, or royalties.

Competing interests disclosure

The authors have no competing interests or relevant affiliations with any organization or entity with the subject matter or materials discussed in the manuscript. This includes employment, consultancies, honoraria, stock ownership or options, expert testimony, grants or patents received or pending, or royalties.

Writing disclosure

No writing assistance was utilized in the production of this manuscript.



References

Papers of special note have been highlighted as: • of interest; •• of considerable interest

- Ebrahimi SB, Samanta D. Engineering protein-based therapeutics through structural and chemical design. Nat. Commun. 14(1), 2411 (2023).
- Leader B, Quentin B, Golan D. Protein therapeutics: a summary and pharmacological classification. Nat. Rev. Drug. Discov. (7), 21–39 (2008).
- Gorzelany J, Souza M. Protein replacement therapies for rare diseases: a breeze for regulatory approval? Sci. Transl. Med. 5(178), 10.1126/scitranslmed.3005007 (2013).
- Patel A, Cholkar K, Mitra AK. Recent developments in protein and peptide parenteral delivery approaches. Ther. Deliv. 5(3), 337–365 (2014).
- Kelly JM, Gross AL, Martin DR, Byrne ME. Polyethylene glycol-b-poly(lactic acid) polymersomes as vehicles for enzyme replacement therapy. Nanomedicine 12(23), 2591–2606 (2017).
- Iqbal S, Blenner M, Alexander-Bryant A, Larsen J. Polymersomes for therapeutic delivery of protein and nucleic acid macromolecules: from design to therapeutic applications. Biomacromolecules 21(4), 1327–1350 (2020).
- 7. Discher DE, Ahmed F. Polymersomes. Annu. Rev. Biomed. Eng. 8, 323–341 (2006).
- A founding source of information on polymersomes; the paper was important to the material choices and evaluation
 procedures used here.
- Zhang A, Jung K, Li A, Liu J, Boyer C. Recent advances in stimuli-responsive polymer systems for remotely controlled drug release. Prog. Polym. Sci. 99, 101164 (2019).
- 9. Kost J, Langer R. Responsive polymeric delivery systems. Adv. Drug Deliv. Rev. 64, 327–341 (2012).
- 10. Meng F, Zhong Z, Feijen J. Stimuli-responsive polymersomes for programmed drug delivery. Biomacromolecules 10(2), 197–209 (2009).
- Wells CM, Harris M, Choi L, Murali VP, Guerra FD, Jennings JA. Stimuli-responsive drug release from smart polymers. J. Funct. Biomater. 10(3), 34 (2019).
- 12. Kaul A, Short WD, Wang X, Keswani SG. Hyaluronidases in human diseases. Int. J. Mol. Sci. 22(6), 3204 (2021).
- 13. Hu Q, Katti PS, Gu Z. Enzyme-responsive nanomaterials for controlled drug delivery. Nanoscale 6(21), 12273–12286 (2014).
- 14. Srinivasarao M, Low PS. Ligand-targeted drug delivery. Chem. Rev. 117(19), 12133-12164 (2017).
- Yu MK, Park J, Jon S. Targeting strategies for multifunctional nanoparticles in cancer imaging and therapy. Theranostics 2(1), 3–44
 (2012).
- van der Meel R, Vehmeijer LJC, Kok RJ, Storm G, van Gaal EVB. Ligand-targeted particulate nanomedicines undergoing clinical evaluation: current status. Adv. Drug Deliv. Rev. 65(10), 1284–1298 (2013).
- 17. Wang M, Thanou M. Targeting nanoparticles to cancer. Pharmacol. Res. 62(2), 90–99 (2010).
- 18. Storr T, Thompson KH, Orvig C. Design of targeting ligands in medicinal inorganic chemistry. Chem. Soc. Rev. 35(6), 534–544 (2006).
- Tan JX, Wang XY, Su XL et al. Upregulation of HYAL1 expression in breast cancer promoted tumor cell proliferation, migration, invasion and angiogenesis. PLOS ONE 6(7), 10.1371/journal.pone.0022836 (2011).
- 20. Yoffou PH, Edjekouane L, Meunier L et al. Subtype specific elevated expression of hyaluronidase-1 (HYAL-1) in epithelial ovarian cancer. PLOS ONE 6(6), 10.1371/journal.pone.0020705 (2011).
- Raj P, Lee SY, Lee TY. Carbon dot/naphthalimide based ratiometric fluorescence biosensor for hyaluronidase detection. *Materials* 14(5), 10.3390/ma14051313 (2021).
- Paruchuri BC, Smith S, Larsen J. Enzyme-responsive polymersomes ameliorate autophagic failure in a cellular model of GM1 gangliosidosis. Front. Chem. Eng. 4, 91 (2022).
- Serves as the basis for the system which our current research paper worked to optimize; much of our study protocol follows
 what was set forth in this paper.
- Meszaros M, Kis A, Kunos L et al. The role of hyaluronic acid and hyaluronidase-1 in obstructive sleep apnoea. Sci. Rep. 10(1), 10.1038/s41598-020-74769-4 (2020).
- Albeiroti S, Ayasoufi K, Hill DR, Shen B, De La Motte CA. Platelet hyaluronidase-2: an enzyme that translocates to the surface upon activation to function in extracellular matrix degradation. *Blood* 125(9), 1460–1469 (2015).
- Zhang L, Bharadwaj AG, Casper A, Barkley J, Barycki JJ, Simpson MA. Hyaluronidase activity of human Hyal1 requires active site acidic and tyrosine residues. J. Biol. Chem. 284(14), 9433–9442 (2009).
- 26. Boedtkjer E, Pedersen SF. The acidic tumor microenvironment as a driver of cancer. Annu. Rev. Physiol. 82, 103-126 (2020).
- Reshetnyak YK, Yao L, Zheng S, Kuznetsov S, Engelman DM, Andreev OA. Measuring tumor aggressiveness and targeting metastatic lesions with fluorescent pHLIP. Mol. Imaging Biol. 13(6), 1146–1156 (2011).
- 28. Feng L, Dong Z, Tao D, Zhang Y, Liu Z. The acidic tumor microenvironment: a target for smart cancer nano-theranostics. *National Sci. Rev.* 5(2), 269–286 (2018).



Research Article Foster, Cakley & Larsen

- 29. Platt FM. Emptying the stores: lysosomal diseases and therapeutic strategies. Nat. Rev. Drug Discov. 17(2), 133–150 (2018).
- Paruchuri BC, Smith S, Larsen J. Enzyme-responsive polymersomes ameliorate autophagic failure in a cellular model of GM1 gangliosidosis. Front. Chem. Eng. 4, 91 (2022).
- Tyler B, Gullotti D, Mangraviti A, Utsuki T, Brem H. Polylactic acid (PLA) controlled delivery carriers for biomedical applications. Adv. Drug Deliv. Rev. 107, 163–175 (2016).
- 32. Casalini T, Rossi F, Castrovinci A, Perale G. A perspective on polylactic acid-based polymers use for nanoparticles synthesis and applications. *Front. Bioeng. Biotechnol.* 7, 259 (2019).
- Lee BM, Park SJ, Noh I, Kim CH. The effects of the molecular weights of hyaluronic acid on the immune responses. Biomater. Res. 25(1), https://doi.org/10.1186/s40824-021-00228-4 (2021).
- 34. Dovedytis M, Liu ZJ, Bartlett S. Hyaluronic acid and its biomedical applications: a review. Eng. Regener. 1, 102-113 (2020).
- 35. Snetkov P, Zakharova K, Morozkina S, Olekhnovich R, Uspenskaya M. Hyaluronic acid: the influence of molecular weight on structural, physical, physico-chemical, and degradable properties of biopolymer. *Polymers (Basel)* 12(8), 10.3390/polym12081800 (2020).
- Review paper that was paramount to explaining and understanding our observed results as we compared the
 impact of hyaluronic acid's molecular weight in our own system specifically.
- 36. Anselmo AC, Mitragotri S. Nanoparticles in the clinic: an update post COVID-19 vaccines. Bioeng. Transl. Med. 6(3), 1–20 (2021).
- 37. Han E, Kim D, Cho Y, Lee S, Kim J, Kim H. Development of polymersomes co-delivering doxorubicin and melittin to overcome multidrug resistance. *Molecules* 28(3), 1087 (2023).
- Tu¨cking KS, Gru¨tzner V, Unger RE, Scho¨nherr H. Dual enzyme-responsive capsules of hyaluronic acid-block-poly(lactic acid) for sensing bacterial enzymes. Macromol. Rapid Commun. 36(13), 1248–1254 (2015).
- 39. Paap MK, Silkiss RZ. The interaction between hyaluronidase and hyaluronic acid gel fillers a review of the literature and comparative analysis. *Plast. Aesthet. Res.* 7, 36 (2020).
- 40. Stern R, Kogan G, Jedrzejas MJ, S'olte's L. The many ways to cleave hyaluronan. Biotechnol. Adv. 25(6), 537–557 (2007).
- Gushulak L, Hemming R, Martin D, Seyrantepe V, Pshezhetsky A, Triggs-Raine B. Hyaluronidase 1 and β-hexosaminidase have redundant functions in hyaluronan and chondroitin sulfate degradation. J. Biol. Chem. 287(20), 16689 (2012).
- Tømmeraas K, Melander C. Kinetics of hyaluronan hydrolysis in acidic solution at various pH values. Biomacromolecules 9(6), 1535–1540 (2008).
- Casalini T, Rossi F, Castrovinci A, Perale G. A perspective on polylactic acid-based polymers use for nanoparticles synthesis and applications. Front. Bioeng. Biotechnol. 7, 259 (2019).
- Sha L, Chen Z, Chen Z, Zhang A, Yang Z. Polylactic acid based nanocomposites: promising safe and biodegradable materials in biomedical field. Int. J. Polym. Sci. 2016, 6869154 (2016).
- Deng C, Xu X, Tashi D, Wu Y, Su B, Zhang Q. Co-administration of biocompatible self-assembled polylactic acid-hyaluronic acid block copolymer nanoparticles with tumor-penetrating peptide-iRGD for metastatic breast cancer therapy. J. Mater. Chem. B 6(19), 3163–3180 (2018).
- 46. Kelly JM, Pearce EE, Martin DR, Byrne ME. Lyoprotectants modify and stabilize self-assembly of polymersomes. *Polymer* 87, 316–322 (2016)
- Casal JA, Cano E, Tutor JC. β-Hexosaminidase isoenzyme profiles in serum, plasma, platelets and mononuclear, polymorphonuclear and unfractionated total leukocytes. Clin. Biochem. 38(10), 938–942 (2005).
- Kelly JM, Bradbury A, Martin DR, Byrne ME. Emerging therapies for neuropathic lysosomal storage disorders. Prog. Neurobiol. 152, 166–180 (2017).
- 49. Chang HY, Sheng YJ, Tsao HK. Structural and mechanical characteristics of polymersomes. Soft Matter 10(34), 6373-6381 (2014).
- Holowka EP, Pochan DJ, Deming TJ. Charged polypeptide vesicles with controllable diameter. J. Am. Chem. Soc. 127(35), 12423–12428 (2005).
- Krook NM, Tabedzki C, Elbert KC et al. Experiments and simulations probing local domain bulge and string assembly of aligned nanoplates in a lamellar diblock copolymer. Macromolecules 52(22), 8989–8999 (2019).
- 52. Gouveia MG, Wesseler JP, Ramaekers J, Weder C, Scholten PBV, Bruns N. Polymersome-based protein drug delivery quo vadis? *Chem. Soc. Rev.* 52(2), 728–778 (2022).
- 53. Joye I, McClements D. Biopolymer-based delivery systems: challenges and opportunities. *Curr. Top Med. Chem.* 16(9), 1026–1039 (2016).
- 54. Furtado D, Bjo"rnmalm M, Ayton S, Bush AI, Kempe K, Caruso F. Overcoming the blood–brain barrier: the role of nanomaterials in treating neurological diseases. *Adv. Mater.* 30(46), e1801362 (2018).
- 55. Buhren BA, Schrumpf H, Bo"lke E, Kammers K, Gerber PA. Standardized *in vitro* analysis of the degradability of hyaluronic acid fillers by hyaluronidase. *Eur. J. Med. Res.* 23(1), 1–6 (2018).



- Kim SW, Oh KT, Youn YS, Lee ES. Hyaluronated nanoparticles with pH- and enzyme-responsive drug release properties. Colloids Surf. B Biointerfaces 116, 359–364 (2014).
- Biomol GmbH. Guide to enzyme unit definitions and assay design (2019).
 www.biomol.com/resources/biomol-blog/guide-to-enzyme-unit-definitions-and-assay-design
- 58. Sigma Aldrich. Hyaluronidase type II, lyophilized powder, main=300units/mg solid 37326-33-3. www.sigmaaldrich.com/US/en/product/sigma/h2126
- 59. Lee JS, Feijen J. Polymersomes for drug delivery: design, formation and characterization. J. Control. Rel. 161(2), 473-483 (2012).
- ISO. 10993-5: 2009 Biological evaluation of medical devices-part 5: tests for in vitro cytotoxicity (2009). www.iso.org/standard/36406.html
- Luckanagul JA, Bhuket PRN, Muangnoi C, Rojsitthisak P, Wang Q, Rojsitthisak P. Self-assembled thermoresponsive nanogel from grafted hyaluronic acid as a biocompatible delivery platform for curcumin with enhanced drug loading and biological activities. *Polymers* (Basel) 13(2), 1–14 (2021).
- Deng C, Xu X, Tashi D, Wu Y, Su B, Zhang Q. Co-administration of biocompatible self-assembled polylactic acid-hyaluronic acid block copolymer nanoparticles with tumor-penetrating peptide-iRGD for metastatic breast cancer therapy. J. Mater. Chem. B 6(19), 3163– 3180 (2018).
- 63. Alipoor R, Ayan M, Hamblin MR, Ranjbar R, Rashki S. Hyaluronic acid-based nanomaterials as a new approach to the treatment and prevention of bacterial infections. Front. Bioeng. Biotechnol. 10, 913912 (2022).
- Gheran CV, Rigaux G, Callewaert M et al. Biocompatibility of Gd-loaded chitosan-hyaluronic acid nanogels as contrast agents for magnetic resonance cancer imaging. Nanomaterials 8(4), 10.3390/nano8040201 (2018).
- 65. Nance EA, Woodworth GF, Sailor KA et al. A dense poly(ethylene glycol) coating improves penetration of large polymeric nanoparticles within brain tissue. Sci. Transl. Med. 4(149), 10.1126/scitranslmed.3003594 (2012).

